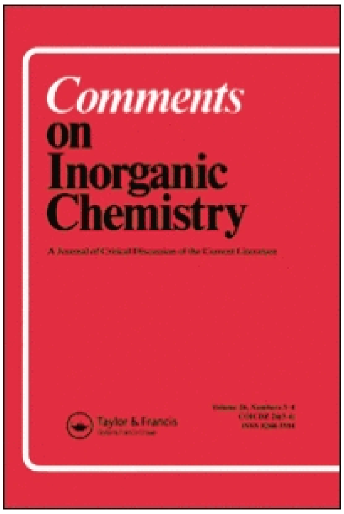

Comments on Inorganic Chemistry
Publication details, including instructions for authors and subscription information:
http://www.informaworld.com/smpp/title~content=t713455155

Diruthenium Metallaynes: Versatile Chromophores and Electrophores

Tong Ren[a]; Guo-Lin Xu[a]
[a] Department of Chemistry, University of Miami, Coral Gables, Florida, USA

To cite this Article Ren, Tong and Xu, Guo-Lin(2002) 'Diruthenium Metallaynes: Versatile Chromophores and Electrophores', Comments on Inorganic Chemistry, 23: 5, 355 — 380

To link to this Article: DOI: 10.1080/02603590215000

URL: http://dx.doi.org/10.1080/02603590215000

Comments on Inorganic Chemistry, 23: 355–380, 2002

0260-3594/02 $12.00 + .00
DOI: 10.1080/02603590290013271

Diruthenium Metallaynes: Versatile Chromophores and Electrophores

Tong Ren and Guo-Lin Xu
Department of Chemistry, University of Miami,
Coral Gables, Florida, USA.

Both the mono- *and* bis-*alkynyl adducts on a diruthenium core supported by either diarylformamidinate, or 2-anilinopyridinate, or dimethylbenzamidinate have been synthesized and characterized. These novel* Ru_2*-metallaynes are highly redox flexible, soluble in common organic solvents and stable towards air, moisture and heat. Electrochemical and spectroscopic studies revealed that the* Ru_2*-metallaynes have exceptionally small solution HOMO-LUMO gaps (1.2–1.4 eV) and high electron affinities.* Ru_2*-metallaynes can be oxidatively coupled at ≡C-H termini, and the resultant dimers exhibit an extensive electronic delocalization across the polyyne-diyl* ($-C_{2m}-$) *bridge. Study of a* bis-*(1-ferrocenylethynyl)-adduct revealed that the* Ru_2 *core facilitates electron transfer between two Fc termini.*

Keywords: metallaynes, diruthenium, chromophores, electrophores, molecular wires

1. INTRODUCTION

The last two decades have witnessed a rapid expansion of the chemistry of metallaynes, metal complexes bearing one or more σ-bonded alkynyl ligands.[1,2] The extensive conjugation along the rigid $M\text{-}(C{\equiv}C)_n\text{-}$ linkage enables metallaynes to exhibit significant optical nonlinearity[3] and function as highly luminescent chromophores.[4] In hoping to achieve an organometallic molecular wire, intensive efforts have been invested in establishing high electron mobility between two metal complexes connected by a polyyne-diyl linker (**I** in Scheme 1).[5–9] While the facile electronic delocalizations across the polyyne-diyl bridge have been verified in all above-mentioned studies,

Received June 14, 2002; Revised July 9, 2002.

Address correspondence to Tong Ren, Department of Chemistry, University of Miami, Coral Gables, FL 33124. E-mail: tren@miami.edu

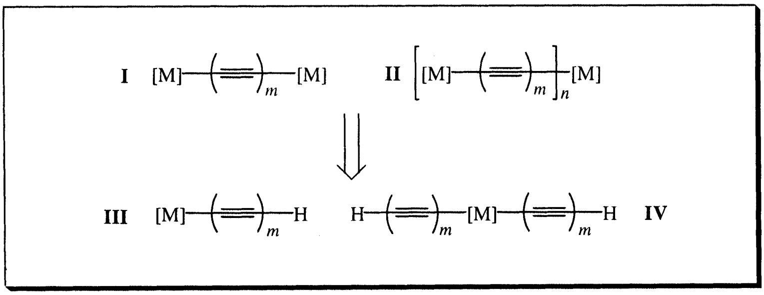

SCHEME 1 Metallayne dimer (**I**), oligomer (**II**), and their mono- (**III**) and difunctional synthons (**IV**).

the scope has been limited to the simple dimer **I**. It is more desirable to construct molecular wires based on an oligo(metallayne) (**II** in Scheme 1), where the length of the wire can be tailored by controlling the degree of oligomerization (*n*). From the structural perspective, synthesis of **II** necessitates both the mono-functional (**III** in Scheme 1) and di-functional (**IV**) metallayne synthons. The predominant motif [M] for the study of **I** has been the $CpML_n$ type complex, which, unfortunately, cannot be derivatized to yield difunctional synthon **IV**. Hence, alternative structural motifs have to be considered as the synthons for oligomer **II**. Besides the structural prerequisite, a small HOMO-LUMO gap and high electron affinity are two key electronic characteristics expected for the synthons of *molecular wires*.[10,11]

While metallayne chemistry has been dominated by mononuclear transition metal complexes, the scope of dinuclear metallaynes has broadened significantly in recent years. The first of such compounds, $Ru_2(ap)_4(C{\equiv}CPh)$ ($ap = $ 2-anilinopyridinate), was obtained through the metathesis reaction between $Ru_2(ap)_4Cl$ and $LiC{\equiv}CPh$ by Cotton and Chakravarty in 1986,[12] where the phenylacetylide ligand occupies the axial position of $Ru_2(ap)_4$ core, as shown in Scheme 2a. Synthesis and structural characterization of a dirhodium analogue, $Rh_2(ap)_4(C{\equiv}CH)$, were reported by Bear *et al.* in 1990.[13] Hopkins and coworkers reported the synthesis and detailed spectroscopic studies of several compounds of the general formula $M_2(PR_3)_4(C{\equiv}CR')_4$ with M as Mo and W in the 90's, where ethynyl ligands occupy the equatorial positions (Scheme 2b).[14] Bear and coworkers demonstrated the possibility of placing phenylacetylides at both axial positions of the Ru_2 core, initially with diphenylformamidinate (D*Ph*F)[15] as the bridging ligand and later with F_5ap (2-pentafluoroanilinepyridinate).[16]

The ability to accommodate two alkynyl ligands in a *trans*-arrangement makes the diruthenium system a promising candidate for difunctional synthons (**IV**). However, the phenylacetylide adducts reported by Bear's[15] and our laboratories[17] exhibit poor thermal stability. In addition,

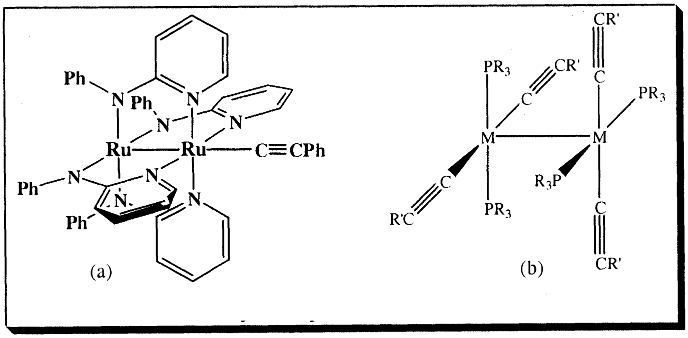

SCHEME 2 Early examples of dinuclear metallaynes.

incorporation of the *bis*-phenylacetylide complexes into an oligomer would require the activation of an aromatic C-H bond, which can be synthetically challenging. In searching for *mono*- and *di*-functional synthons that are both highly stable and amenable to covalent coupling chemistry, we began to explore polyynyl complexes of the diruthenium compounds supported by *N*,*N′*-bidentate bridging ligands in early 1999, and the results obtained are summarized here. The *N*, *N′*-bidentate bridging ligands utilized include both the *N*,*N′*-diarylformamidinates (*D*Ar*F*), 2-anilinopyridinate (*ap*) and *N*,*N′*-dimethylbenzamidinate (*DMBA*) (Scheme 3).[18]

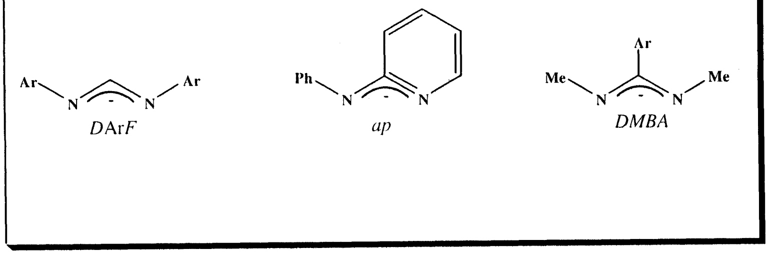

SCHEME 3 *Mono*- and *bis*-alkynyl adducts on a Ru_2 core, and the supporting *N*,*N′*-ligands employed.

2. RU$_2$(*D*AR*F*)$_4$-BASED METALLAYNES

Earlier work demonstrated that treating $Ru_2(DArF)_4Cl$, a Ru_2(II, III) species, with excess (>20 equivalents) LiC≡CPh yielded either $Ru_2(DArF)_4(C{\equiv}CPh)$, if the solvent removal was carried out *in vacuo*, or *trans*-$Ru_2(DArF)_4(C{\equiv}CPh)_2$, a Ru_2(III, III) compound, if the solution was stirred in air prior to the solvent removal.[15,17] This peculiar behavior can be explained by a solution equilibrium between $Ru_2(DArF)_4(CCPh)$ and [*trans*-$Ru_2(DArF)_4(CCPh)_2]^{1-}$ in the presence of excess LiCCPh:

$$[Ru_2]Cl \xrightarrow{LiC_2Ph} [Ru_2](C_2Y) \underset{}{\overset{excess\, LiC_2Ph}{\rightleftharpoons}} \{[Ru_2](C_2Y)_2\}^{1-} \quad (1)$$

These phenylethynyl adducts are highly soluble in common organic solvents and exhibit multiple one electron redox processes (see discussion below).[15,17] However, they are thermally unstable, which significantly limits the possibility of material applications.

Similar to the synthesis of phenylethynyl adducts, treating $Ru_2(DmAniF)_4Cl$ (*D*mAni*F* is di(*m*-methoxyphenyl)formamdinate) with three equivalent of LiC_4SiMe_3 led to the formation of both $Ru_2(DmAniF)_4(C_4SiMe_3)$(42% purified yield) and *trans*-$Ru_2(DmAniF)_4(C_4SiMe_3)_2$ (28% purified yield).[19] In contrast with the case of phenylethynyl adducts, the ratio between *mono*- and *bis*-butadiynyl adducts is independent of work-up conditions. Similar results were also obtained with Ru_2 compounds supported by both *m*-Cl and *m*-CF_3 substituted formamidinates.[20] Further corroborating the existence of the above-mentioned equilibrium, Lehn and coworkers reported that treating $Ru_2(DPhF)_4Cl$ (*D*Ph*F* is diphenylformamdinate) with 22 equivalents of LiC_4SiMe_3 yielded *trans*-$Ru_2(DPhF)_4(C_4SiMe_3)_2$ (70%) as the only isolated product.[21] More recently, Kuhn *et al.* reported that treating $Ru_2(DArF)_4Cl$ with an excess of LiC_2-4-py also led to the isolation of the *bis*-compound *trans*-$[Ru_2(DArF)_4](C_2\text{-4-py})_2$.[22] Alternatively, the stoichiometric metathesis of the axial chloro ligand by a polyynyl ligand can be achieved with a trimethylstannyl alkynyl agent under Stile coupling conditions (Eq. 2), where only the *mono*-polyynyl adduct was isolated.[20]

$$Ru_2(DmAniF)_4Cl \xrightarrow[Pd(PPh_3)_2Cl_2,CuI]{1eq.\ Me_3SnC_6SiMe_3} Ru_2(DmAniF)_4(C_6SiMe_3)(50\%) \quad (2)$$

All *mono*-alkynyl adducts are Ru_2(II, III) compounds of $S = 3/2$, while all *bis*-adducts are Ru_2(III, III) compounds and diamagnetic. In contrast to the phenylacetylide analogs, the polyynyl complexes with silyl group intact exhibit high stability towards heat (up to 80°C in an ambient atmosphere), moisture, and air. These compounds are soluble in common organic solvents, including hexanes. Both the *mono*- and *bis*-polyynyl adducts on $Ru_2(DArF)_4$ core are highly crystalline materials and several single crystal X-ray

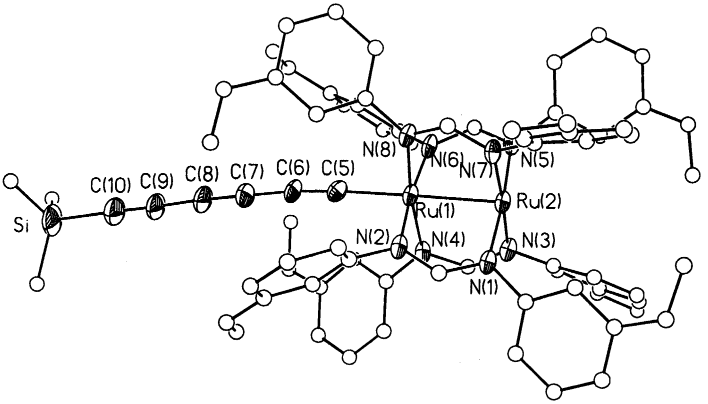

FIGURE 1 ORTEP plot of $Ru_2(\mathit{Dm}AniF)_4(C_6SiMe_3)$ at 30% probability level.

diffraction studies have been completed. Structural plots of $Ru_2(\mathit{D}mAniF)_4(C_6SiMe_3)$, *trans*-$Ru_2(\mathit{D}mAniF)_4(C_4SiMe_3)_2$, and *trans*-$Ru_2(\mathit{Dm}ClPhF)_4(C_4SiMe_3)_2$ are shown in Figures 1, 2 and 3, respectively. These compounds have an overall shape of a cylinder, and the Ru-Ru-polyynyl backbones are approximately collinear with the axis of the cylinder.

Table 1 lists the selected topological parameters around the Ru_2-core determined for $Ru_2(\mathit{D}ArF)_4$-based compounds, where several trends are clear. While isoelectronic to the parent compounds $Ru_2(\mathit{D}ArF)_4Cl$,[23,24] *mono*-alkynyl compounds exhibit longer Ru-Ru bond, which is attributed to the strong σ-donor nature of alkynyl ligands. Upon the formation of the *bis*-alkynyl adduct, the d_{z^2} orbital on each Ru center is mainly involved in the

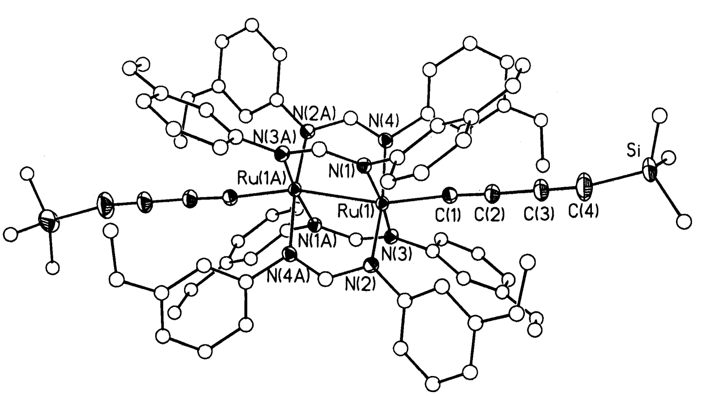

FIGURE 2 ORTEP plot of $Ru_2(\mathit{Dm}AniF)_4(C_4SiME_3)_2$ at 30% probability level.

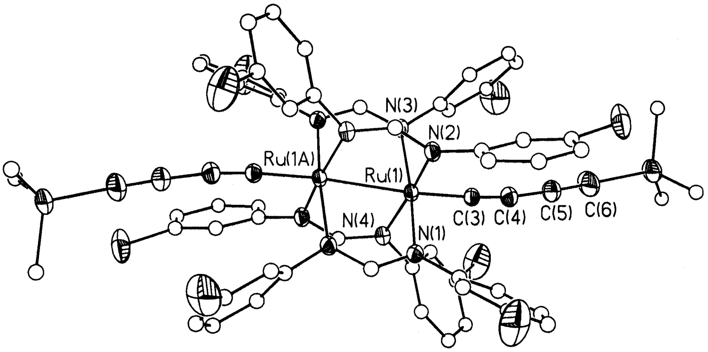

FIGURE 3 ORTEP plot of $\mathrm{Ru_2}(D m\mathrm{ClPh}F)_4(\mathrm{C_4SiMe_3})_2$ at 30% probability level.

TABLE 1 Key Geometrical Parameters of $\mathrm{Ru_2}(D\mathrm{Ar}F)_4(\mathrm{C_2Y})_\mathrm{n}$ ($n = 1$ and 2)

	Ru-Ru	$\mathrm{Ru\text{-}C}_{av.}$	$\mathrm{Ru\text{-}N}_{av.}$	$\mathrm{C_\alpha\text{-}C_\beta}$	$\mathrm{Ru\text{-}Ru\text{-}C_\alpha}$
$n = 1$					
$\mathrm{Ru_2}(D\mathrm{Ph}F)_4(\mathrm{C_2Ph})^{15}$	2.400[1]	2.028[7]	2.076[4]	1.214[11]	180.0
$\mathrm{Ru_2}(D m\mathrm{ClPh}F)_4$-$(\mathrm{C_2Ph})^{20}$	2.3868(10)	2.057(9)	2.082[6]	1.191(11)	180.0
$\mathrm{Ru_2}[D(3,5\text{-}\mathrm{Cl_2Ph})F]_4$-$(\mathrm{C_2Ph})^{17}$	2.4285(11)	2.036(9)	2.058[6]	1.197(12)	180.0
$\mathrm{Ru_2}(D\mathrm{mAni}F)_4$-$(\mathrm{C_4SiMe_3})^{19}$	2.5060(5)	2.027(5)	2.046[3]	1.207(6)	175.34(12)
$\mathrm{Ru_2}(D\mathrm{mAni}F)_4$-$(\mathrm{C_6SiMe_3})^{20}$	2.4936(8)	2.015(7)	2.036[6]	1.228(9)	179.1(2)
$n = 2$					
$\mathrm{Ru_2}(D\mathrm{Ph}F)_4$-$(\mathrm{C_2Ph})_2{}^{15}$	2.553(1)	1.987[8]	2.055[11]	1.178[11]	159.7[3]
$\mathrm{Ru_2}(D p\mathrm{ClPh}F)_4$-$(\mathrm{C_2Ph})_2{}^{17}$	2.5554(12)	1.991[5]	2.054[4]	1.195[7]	158.8[2]
$\mathrm{Ru_2}(D\mathrm{mAni}F)_4$-$(\mathrm{C_4SiMe_3})_2{}^{19}$	2.5990(3)	1.947[2]	2.056[2]	1.206[3]	164.34[7]
$\mathrm{Ru_2}(D m\mathrm{ClPh}F)_4$-$(\mathrm{C_4SiMe_3})_2{}^{20}$	2.5600(4)	1.970[3]	2.060[2]	1.211[4]	158.29[8]
$trans\text{-}\mathrm{Ru_2}(D p\mathrm{tol}F)_4$-$(\mathrm{C_2pyRe(CO)_3}$-$(t\text{-}\mathrm{Bubipy}))_2{}^{22}$	2.5664(4)	1.961(4)	2.048[3]	1.204(6)	161.12(10)

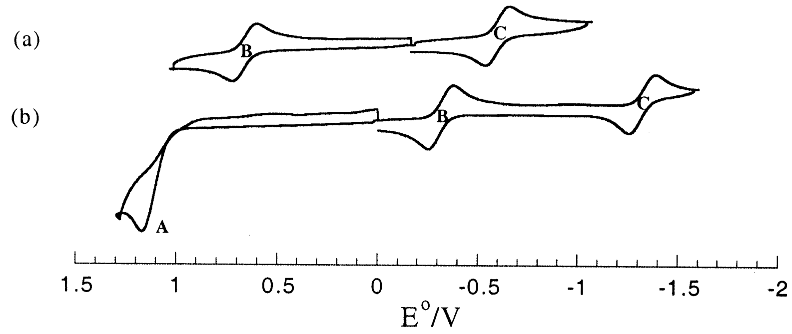

FIGURE 4 CVs of $Ru_2(DmAniF)_4(C_4SiMe_3)$ (a) and $Ru_2(DmAniF)_4(C_4SiMe_3)_2$ (b).

formation of the σ(Ru-C_α) bond and the σ(Ru-Ru) bond no longer exists. Hence, the *bis*-alkynyl compounds have the longest Ru-Ru bond among Ru_2-paddlewheel compounds.[25] The Ru-Ru-C_α bond angles in the *bis*-adducts deviate significantly from linearity, while none or insignificant deviations were observed for the *mono*-adducts. Both the bending of Ru-Ru-C_α angle and large variation among Ru-N bond lengths (not shown in Table 1) are attributed to a second order Jahn-Teller distortion based on the Fenske-Hall calculations.[17] Due to the electron-deficiency of the C≡C bond,[26] the polyynyl ligand is more electronic withdrawing than phenylethynyl ligand. Compared with the phenylethynyl adducts, the polyynyl adducts exhibit both the elongation of the Ru-Ru bond and shortening of the Ru-C_α bond, indicating the enhancement of the Ru-C_α π-bonding at the expense of the Ru-Ru π-bonding. Recent structural determination of *trans*-$[Ru_2(DpTolF)_4](C_2Y)_2$ with Y as $(4\text{-py})Re(CO)_3({}^tBu_2bipy)$ revealed geometrical features around the Ru_2 core similar to those of $[Ru_2(DArF)_4](C_2Ph)_2$.[22]

Both the *mono*- and *bis*-alkynyl compounds are redox rich, and exhibit multiple (quasi)reversible one-electron processes. An oxidation and a reduction are commonly observed for the *mono*-adducts, while one oxidation (irreversible) and two reductions are observed for the *bis*-adducts, as shown in Figure 4. Designation of these couples is provided in Eq. (3):

$$\underset{\text{A}}{Ru_2(IV,III)\underset{+e^-}{\overset{-e^-}{\rightleftarrows}}}Ru_2(III,III)\underset{\text{B}}{\underset{-e^-}{\overset{+e^-}{\rightleftharpoons}}}Ru_2(II,III)\underset{\text{C}}{\underset{-e^-}{\overset{+e^-}{\rightleftharpoons}}}Ru_2(II,II) \quad (3)$$

Availability of electrode potentials for both the one-electron oxidation and reduction couples enables the estimation of the HOMO-LUMO gap (E_g) for these Ru_2-metallaynes according to the following relationship:[27,28] $E_g = E_{1/2}(+1/0) - E_{1/2}(0/-1)$. In the case of mono-alkynyl species, the E_g values are within a narrow range of 1.22–1.26 V. For the *bis*-alkynyl species, the E_g values range from 1.34–1.49 V, where the larger variation could be attributed to the irreversibility of couple **A**.

A noteworthy feature revealed by voltammetric studies is the $E_{1/2}$(**B**) of *bis*-alkynyl species: it is far more positive than the reduction potential of O_2 (*ca.* – 0.90 V in THF under experimental conditions). In other words, the (first) electron affinity (*EA*) of the *bis*-species is much larger than that of O_2 molecule. Consequently, oxygen/air cannot oxidize the oligo(Ru_2-metallayne) carrying up to one electron per monomer and the *molecular wire* will be air stable at the conducting state.

As revealed by the Vis-NIR (visible-near-infrared) absorption spectra of $Ru_2(D\mathrm{mClPh}F)_4(C_2Ph)_x$ in Figure 5 ($x = 1$ and 2), both the *mono*- and *bis*-alkynyl compounds exhibit an intensive charge-transfer band with the onset around 800 nm and peak between 500–550 nm, which accounts for the characteristic deep red/purple appearance for these compounds. In addition, weak absorptions in the NIR region are observed as a well-defined peak for the *bis*-adduct and a shoulder for the *mono*-adduct (insert in Figure 5). The optical gaps calculated from the λ_{max} of the lowest energy absorption ($E_{op}/\mathrm{eV} = 10^7/(8066\lambda_{max})$) are also listed in Table 4, where it is clear that

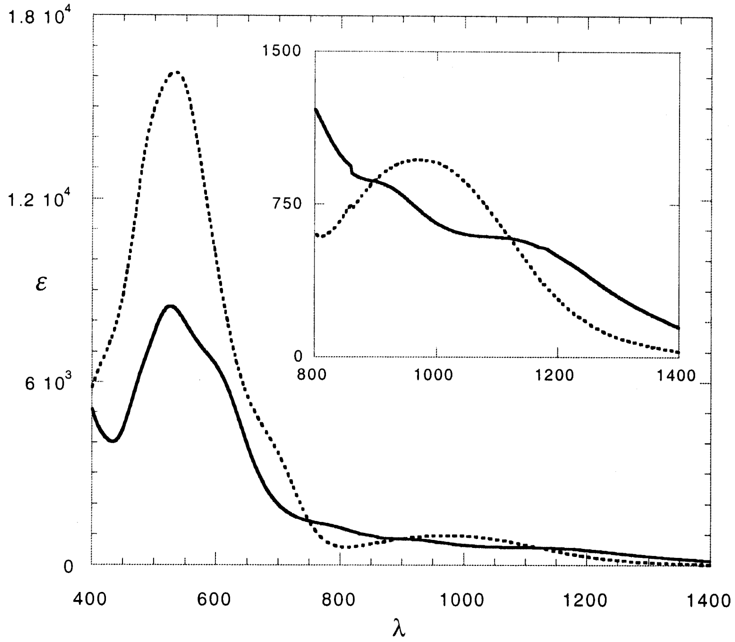

FIGURE 5 Vis-NIR absorption spectra of $Ru_2(D\mathrm{mClPh}F)_4(C_2Ph)_x$ in THF, solid: $x = 1$, dash: $x = 2$.

the E_{op}s are slightly smaller than the E_{g}s. Obtaining monomers with small HOMO-LUMO gaps, known as *bandgap engineering*, is a key step in optimizing the electronic and optoelectronic properties of conjugated oligomers.[11] The ramification of the remarkably small HOMO-LUMO gaps observed here remains to be explored.

3. RU$_2$(*AP*)$_4$-BASED METALLAYNES

In the original work of Chakravarty and Cotton,[12] treatment of $Ru_2(ap)_4Cl$ with five equivalent of LiC_2Ph produced $Ru_2(ap)_4(C_2Ph)$ as the only product in 70% yield. However, the excess of LiC_2Ph appears unnecessary since $Ru_2(ap)_4(C_2Y)$ type compounds were isolated by treating $Ru_2(ap)_4Cl$ with one equivalent of LiC_2Y with Y as $SiMe_3$, Si^iPr_3 and CH_2OCH_3.[29,30] On the other hand, reaction between $Ru_2(F_5ap)_4Cl$ and fifty equivalent of LiC_2Ph resulted in both $Ru_2(F_5ap)_4(C_2Ph)$ (40%) and *trans*-$[Ru_2(F_5ap)_4](C_2Ph)_2$ (40%).[16] More recently, we disclosed that *trans*-$[Ru_2(ap)_4](C_2Ph)_2$ became the dominant product (70%) when twenty equivalent of LiC_2Ph was used.[31] These results are consistent with the equilibrium indicated in Eq. (1). Treating $Ru_2(ap)_4Cl$ with five equivalent of LiC_4SiMe_3 also led to the formation of both $Ru_2(ap)_4(C_4SiMe_3)$ and *trans*-$Ru_2(ap)_4(C_4SiMe_3)_2$, but the ratio between *mono*- and *bis*-adducts strongly depends on workup conditions.[32] Purification after the solvent removal *in vacuo* resulted in a 3:1 ratio, while stirring the reaction mixture in air prior to purification gave an inverted ratio (1:3). Alkynylation of Ru_2L_4 core (L = *ap* and 2-halooxypyridinate) under Stille coupling conditions yielded corresponding *mono*-alkynyl compounds.[33]

$$Ru_2L_4Cl + Me_3SnC_2Ph \xrightarrow{cat.\mathrm{Pd(II)/CuI}} Ru_2L_4(C_2Ph) \qquad (4)$$

In contrast to the cases involving either phenylethynyl or linear polyynyls, $Ru_2(ap)_4(C_2SiR_3)$ (R = Me and ^{i}Pr) remains the only product when the stoichiometry of LiC_2SiR_3 is increased from one to ten.[30] Absence of the *bis*-adduct is due to the bulkiness of silyl groups, which prevents acetylide from accessing the axial position flanked by anilino groups, a property attributed to the unique (4,0)-arrangement of *ap* ligands (see discussion below). However, access to the same axial position is not prohibited when either phenylacetylide or silyl-capped butadiynyl is used. Thus, reacting $Ru_2(ap)_4(C_2SiR_3)$ with six equivalent of LiC_4SiMe_3 led to the isolation of *trans*-$(Me_3SiC_4)[Ru_2(ap)_4](C_2SiR_3)$,[30] and reacting $Ru_2(ap)_4(C_2Y)$ (Y = $SiMe_3$ and C_2SiMe_3) with twenty equivalent of LiC_2Ph yielded *trans*-$(PhC_2)[Ru_2(ap)_4](C_2Y)$.[31] Due to a higher electron deficiency of the butadiynyl group, the C_4SiMe_3 group in *trans*-(Me_3SiC_4) $[Ru_2(ap)_4](C_2SiR_3)$ is more susceptible to nucleophilic attack than the C_2SiR_3 group and can be selectively removed using K_2CO_3 to give *trans*-$(HC_4)[Ru_2(ap)_4](C_2SiR_3)$, a potential orthogonal synthon for oligo(metallaynes).[30] In the case of R = Me, the ethynyl silyl can be removed by treating *trans*-(Me_3SiC_4)[Ru_2(*ap*)$_4$](C_2SiMe_3) with NaOH to yield *trans*-(HC_4)[Ru_2(*ap*)$_4$](C_2H).[30]

While the transmetallation reaction between [Ru_2]Cl and $M'C_{2m}R$ (M' = Li and SnR'_3) has been successful in preparing [Ru_2]($C_{2m}R$) with short polyynyl ligands ($m \leq 3$), its utility in preparing [Ru_2]($C_{2m}R$) with $m \geq 4$ becomes very limited due to increasing thermal instability of $HC_{2m}R$ with increasing *m*. Typically, metallaynes bearing longer polyynyl are prepared by the *Cadiot-Chodkiewicz* reaction between [M]-$C_{2m}Cu$ and $BrC_{2n}R$.[10,34] The utility of this reaction was elegantly demonstrated by Gladysz *et al.*, who obtained {Re}($C_{2m}R$) with *m* up to five ({Re} = ($\eta^{[5]}$-C_5Me_5)Re(NO)(PPh_3), R = H and $SiMe_3$).[35] Taking advantage of the extraordinary air and moisture stability of Ru_2(*ap*)$_4$($C_{2m}H$), we succeeded in extending the Ru_2-metallayne by a cross-coupling reaction between [Ru_2(*ap*)$_4$](C_4H) and HC_2Y (Y = SiR_3, CH_2OCH_3, Ph and Fc) under *Hay* conditions, as shown in Scheme 4.[36] The yield of the extended metallayne **4b** can be optimized by the addition of excess organic alkyne HC_2Y. Furthermore, the product [Ru_2(*ap*)$_4$](C_6SiR_3) can be easily de-silylated to yield [Ru_2(*ap*)$_4$](C_6H), which undergoes cross coupling reaction to yield [Ru_2(*ap*)$_4$](C_8Y).[20] Hence, the cross coupling under *Hay* conditions is a viable substitute of the *Cadiot-Chodkiewicz* reaction in obtaining longer metallayne.

The Ru_2(*ap*)$_4$-based metallaynes can be readily crystallized, and a few selected structures are shown in Figures 6–8, while the relevant bond lengths and angles are collected in Table 2 for all known structures. The *ap* ligands in all of these compounds adopt the so-called (4,0)-arrangement around the Ru_2 center: all the pyridine *N*-centers coordinate to the same ruthenium center (Ru1) while all anilino *N*-centers coordinate to the other (Ru2). The axial position at Ru1 is much less hindered than that at Ru2, and consequently the alkynyl ligand bonds to Ru1 in all *mono*-alkynyl compounds. The deep pocket formed by the anilino groups flanking Ru2 enforces a selectivity on the alkynyl ligand in forming the *bis*-adducts: C_2SiR_3 cannot access Ru2 and hence the *mono*-adduct is the only product regardless the ratio of LiC_2SiR_3 to

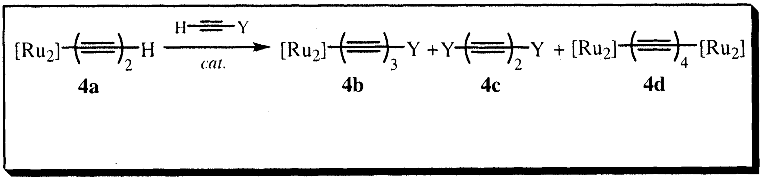

SCHEME 4 Metallayne extension *via* cross coupling under *Hay* conditions (*cat.* CuCl/TMEDA, O_2).

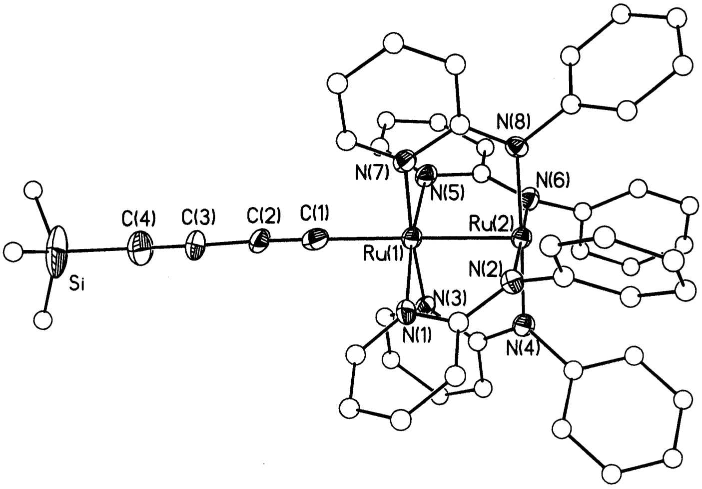

FIGURE 6 ORTEP plot of $Ru_2(ap)_4(C_4SiMe_3)$ at 30% probability level.

$[Ru_2]$, while both polyynyl ($C_{2m}Y$, $m \geq 2$) and C_2Ph can access Ru2 and the *bis*-adduct forms when the alkynyl ligand is supplied in excess.

The *mono*-alkynyl compounds exhibit a relatively constant Ru-Ru distance around 2.325 Å, which is about 0.05 Å longer than that of the parent compound $Ru_2(ap)_4Cl$ (2.275(3) Å).[37] It is interesting to note that the replacement of the *ap* bridge with the more electron deficient F_5ap ligand

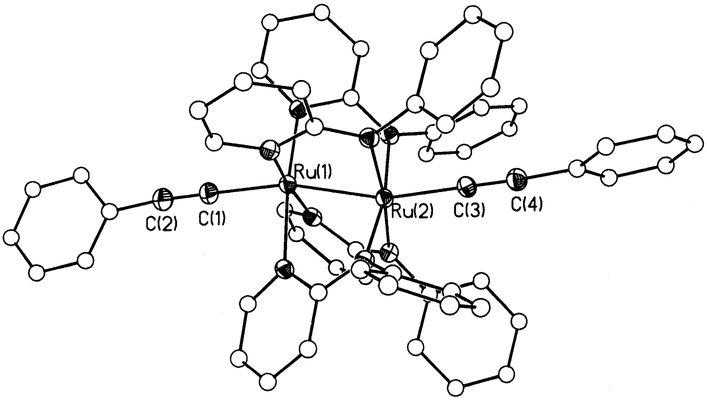

FIGURE 7 ORTEP plot of $Ru_2(ap)_4(C_2Ph)_2$ at 30% probability level.

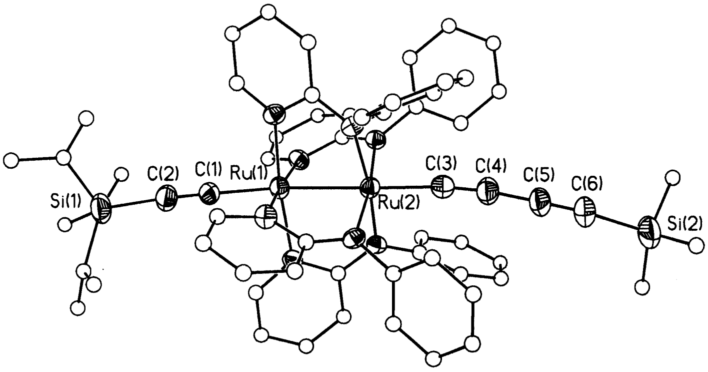

FIGURE 8 ORTEP plot of *trans*-$(Me_3SiC_4)[Ru_2(ap)_4](C_2Si^iPr_3)$ at 30% probability level.

resulted in an insignificant 0.016 Å increase in the Ru-Ru distance.[12,16] Constant Ru-C_α distance (2.08 Å) is also observed with the exception of $Ru_2(ap)_4(C_2CH_2OCH_3)$ and $Ru_2(F_5ap)_4(C_2Ph)$, where severe disorder of the ethynyl ligands prevent a precise determination of the related parameters.

TABLE 2 Key Geometrical Parameters of $Ru_2(ap)_4(C_2Y)_n$ ($n = 1$ and 2)

	Ru-Ru	Ru-$C_{av.}$	Ru-$N_{av.}$	C_α-C_β	Ru-RU-C_α
$n = 1$					
$Ru_2(ap)_4(C_2Ph)^{12}$	2.319(3)	2.08(3)	2.066[17]	1.14(3)	178.0(8)
$Ru_2(ap)_4(C_2SiMe_3)^{29}$	2.3162(5)	2.077(4)	2.071[2]	1.207(6)	180.0
$Ru_2(ap)_4$-$(C_2CH_2OCH_3)^{29}$	2.3234(7)	2.139(7)	2.065[5]	1.144(16)	179.0(2)
$Ru_2(ap)_4(C_4SiMe_3)^{32}$	2.3303(9)	2.075(9)	2.078[7]	1.207(11)	178.5(3)
$Ru_2(ap)_4(C_6H)^{36}$	2.3277(6)	2.076(8)	2.063[3]	1.211(11)	180.0
$Ru_2(F_5ap)_4(C_2Ph)^{16}$	2.335(1)	2.096(7)	2.075[3]	1.178(11)	180.0
$n = 2$					
$Ru_2(ap)_4(C_2Ph)_2{}^{31}$	2.4707(3)	1.988[2]	2.0618[18]	1.204[3]	162.99[7]
$Ru_2(ap)_4(C_2SiMe_3)_2{}^{32}$	2.4717(11)	1.947[10]	2.037[8]	1.222[13]	163.5[3]
trans-(Me_3SiC_4)-$[Ru_2(ap)_4](C_2Si^iPr_3)^{30}$	2.4584(6)	1.966[5]	2.060[4]	1.198[6]	176.43[16]
trans-(HC_4)-$[Ru_2(ap)_4](C_2SiMe_3)^{30}$	2.4662(3)	1.969[3]	2.056[2]	1.210[4]	165.08[8]
trans-(PhC_2)-$[Ru_2(ap)_4](C_4SiMe_3)^{31}$	2.4342(8)	1.966[7]	2.061[4]	1.168[10]	180.0
$Ru_2(F_5ap)_4(C_2Ph)_2{}^{16}$	2.441(1)	1.953[12]	2.068[7]	1.212[23]	171.4[3]

The Ru-Ru-C_α angle is almost, if not exactly, linear. Both the structural features around the first coordination sphere of the Ru_2 core and the $S = 3/2$ spin state indicate that the *mono*-alkynyl adducts are isoelectronic to the parent compound $Ru_2(ap)_4Cl$.[25]

The Ru-Ru bond length in the *bis*-alkynyl adducts ranges from 2.434–2.472 Å and has a mean value of 2.457 Å, a 0.132 Å increment from the *mono*-alkynyl species. Compared with the *mono*-species, the Ru-C_α bond length in the *bis*-species is shortened by *ca.* 0.1 Å. A significantly enhanced Ru-C_α σ-bond largely contributes to the shortening, while the change in covalent radii from $Ru^{+2.5}$ to Ru^{+3} contributes to a lesser degree, as reflected by an insignificant shortening of the Ru-N bond length from the *mono*- to *bis*-species. Most of the *bis*-species, similar to those supported by *D*Ar*F* bridges, exhibit both large variation among the Ru-N distances and bent Ru-Ru-C_α angles, indicating that second order Jahn-Teller effect is operative. Interestingly, the distortion is minimized in *trans*-$(Me_3SiC_4)[Ru_2(ap)_4](C_2Si^iPr_3)$, illustrating the suppression of the second order Jahn-Teller effect by the bulkiness of Si^iPr_3 group.[30] Furthermore, the distortion is absent in the structure of *trans*-$(PhC_2)[Ru_2(ap)_4](C_4SiMe_3)$ due to the restriction of crystallographic symmetry.[31]

Ru_2-metallaynes based on the *ap* bridge exhibit redox characteristics resembling that of the *D*Ar*F* based compounds: two (quasi)reversible one electron couples (**B** and **C** in Eq. 3) for the *mono*-adducts and three one electron couples (**A**, **B** and **C**) for the *bis*-adducts. As shown by the potential data listed in Table 4, nearly constant $E_{1/2}$ values have been obtained for the $Ru_2(ap)_4(C_2Y)$ type compounds with $Y = H$, $SiMe_3$, Ph, CH_2OCH_3 in CH_2Cl_2.[29] The insensitivity of $E_{1/2}$ towards Y is consistent with the fact that all the redox couples are localized on the Ru_2 core. Availability of the polyynyl compounds $Ru_2(ap)_4(C_{2m}Y)$ ($m = 1-4$, $Y = SiR_3$ and Ph) enables the study of their electrode potentials as the function of the number of acetylene units (m). It is apparent from Table 4 that both the $E_{1/2}$(**B**) and $E_{1/2}$(**C**) shift anodically with the increasing m, and the shift of the latter couple is much more pronounced. It can be inferred hence that the LUMO of the metallayne contains a significantly higher polyynyl contribution than the HOMO.

Similar to the *mono*-alkynyl species, the *bis*-alkynyl species of the most positive potentials, $Ru_2(ap)_4(C_4SiMe_3)_2$, as the most acetylenic units (4), while the least positive species, $Ru_2(ap)_4(C_2Ph)_2$ and *trans*-$(PhC_2)[Ru_2(ap)_4](C_2SiMe_3)$, have the fewest acetylenic units (2). In spite of the difference in both the alkynyl capping group and number of acetylenic units, the *ap*-based *bis*-species exhibit similar E_gs, ranging from 1.14 to 1.22 V.

As typified by the Vis-NIR spectra of $Ru_2(ap)_4(C_2Si^iPr_3)$, *trans*-$(Me_3SiC_4)[Ru_2(ap)_4](C_2Si^iPr_3)$, and $(HC_4)[Ru_2(ap)_4](C_2H)$ shown in Figure 9, the *ap*-based mono-alkynyl adducts exhibit two intense bands around 470 and 740 nm, and are deep green-brown colored, whereas the *bis*-adducts exhibit bands around 440, 480, 650 and 1030 nm, and are deep blue

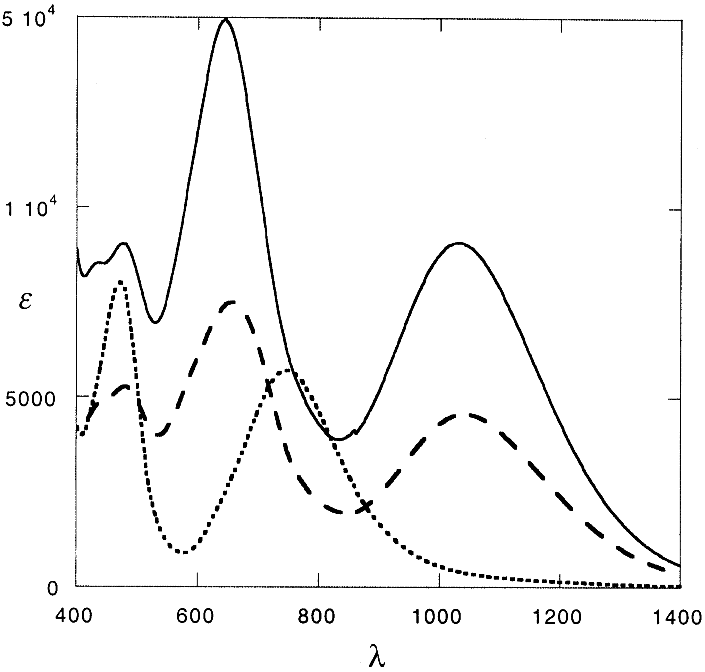

FIGURE 9 Vis-NIR of $Ru_2(ap)_4C_2Si^iPr)$ (dot), *trans*-$(Me_3SiC_4)[Ru_2(ap)_4](C_2Si^iPr)$ (dash), and $(HC_4)[Ru_2(ap)_4](C_2H)$ (solid).

in color. The NIR band observed around 1030 nm for the *bis*-adducts is very intense, and the corresponding E_{op}, 1.20 ± 0.01 eV, agrees well with the E_g values from voltammetric study. On the other hand, careful examination of the NIR absorptions of the *mono*-alkynyl species did not reveal any peak or shoulder. Thus, the E_g of the mono-alkynyl is about 0.4 eV smaller than its E_{op}, and the origin of this discrepancy is not understood presently.

4. RU$_2$(*DMBA*)$_4$-BASED METALLAYNES

In Ru_2-metallaynes based on either the *D*Ar*F* or *ap* bridging ligands, the presence of aryl groups flanking the axial positions of the Ru_2 core necessitates the use of butadiynyl or longer polyynyl ligands in achieving the difunctional building blocks (**IV**). Consequently, the oligomer **II** derived from the coupling of these building blocks will have a polyyne-diyl bridge with a minimum of four C≡C bonds. Since the electronic coupling generally decays exponentially as the length of the bridge increases,[38] use of shorter polyyne-diyl bridges is desired for achieving a higher degree of electronic delocalization. Hence, availability of difunctional modules bearing axial ethynyl ligands is significant in this regard. *N,N'*-Dimethylbenzamidinate (*DMBA*, Scheme 3) appears to exert a minimum steric effect around the axial positions and hence is appealing for the ethynyl-based difunctional modules. In addition, derivatives of *DMBA* with aryls bearing various substituents can be readily prepared, which enable the tuning of both the solubility and electronic properties of the Ru_2-metallaynes.

The first of diruthenium-*DMBA* compounds were unveiled recently,[39] where refluxing $Ru_2(OAc)_4Cl$ with *N,N'*-dimethylbenzamidine resulted in $Ru_2(DMBA)_4Cl_2$ instead of the anticipated $Ru_2(DMBA)_4Cl$. Treating $Ru_2(DMBA)_4Cl_2$ with $M'C_2Y$ ($M' = Li$ and Na) readily afforded the *bis*-alkynyl adducts $Ru_2(DMBA)_4(C_2Y)_2$ ($Y = SiMe_3$, H, Ph, C_2SiMe_3, C_2H and Fc) in nearly quantitative yields, while various attempts to isolate a *mono*-alkynyl adduct have failed.[39] Unique to the *DMBA*-based compounds, the axial chloro ligands can be easily replaced by a weakly coordinating anion (X) such as BF_4^- or NO_3^-. The resultant complex $Ru_2(DMBA)_4X_2$ readily reacts with alkynes in the presence of Et_3N to yield $Ru_2(DMBA)_4(C_2Y)_2$ ($Y = Ph$ and SiR_3).[20] The similarity in reaction conditions to the base-assisted alkynylation of mononuclear $Ru(P\text{-}P)_2$ complexes[40] suggests that the formation of $Ru_2(DMBA)_4(C_2Y)_2$ may be preceded by an Ru_2-vinylidene intermediate, and a plausible mechanism is provided in Scheme 5. Nonetheless, more thorough studies are needed to gain mechanistic insight, especially considering that a highly charged Ru_2^{8+} intermediate is implied by the mechanism outlined in Scheme 5.

Both the parent molecule $Ru_2(DMBA)_4Cl_2$ and the anion metathesis derivatives $Ru_2(DMBA)_4X_2$ are $S = 1$ molecules. Crystal structure analysis revealed that the Ru-Ru bond lengths range from 2.26–2.32 Å (Table 3),

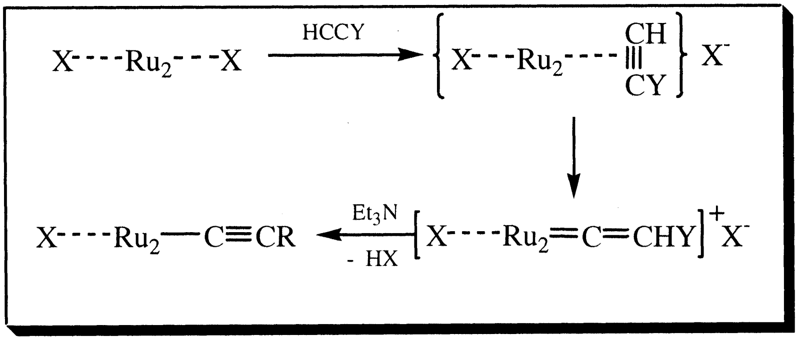

SCHEME 5 Base-assisted alkynylation at $Ru_2(DMBA)_4$ core.

TABLE 3 Key Geometrical Parameters of $\mathrm{Ru_2}(DMBA)_4\mathrm{X_2}$ and $\mathrm{Ru_2}(DMBA)_4(\mathrm{C_2Y})_2$

	Ru-Ru	Ru-N$_{av.}$	Ru-X	Ru-Ru-X	
$\mathrm{Ru_2}(DMBA)_4\mathrm{Cl_2}^{a39}$	2.3228(6)	2.042(2)	2.557(1)	180	
$\mathrm{Ru_2}(DMBA)_4(\mathrm{BF_4})_2{}^{b20}$	2.2646(6)	2.031[4]	2.378[3]	179.57[8]	
$\mathrm{Ru_2}(DMBA)_4(\mathrm{NO_3})_2{}^{c20}$	2.2865(4)	2.037[2]	2.322(2)	176.24(6)	
	Ru-Ru	Ru-C$_{av.}$	Ru-N$_{av.}$	C$_\alpha$-C$_\beta$	Ru-Ru-C$_\alpha$
$\mathrm{Ru_2}(DMBA)_4$-$(\mathrm{C_2SiMe_3})_2{}^{39}$	2.4501(6)	1.955(4)	2.046[3]	1.207(6)	174.8(1)
$\mathrm{Ru_2}(DMBA)_4(\mathrm{C_4H})_2{}^{39}$	2.4559(6)	1.952[5]	2.045[4]	1.206[6]	170.5[1]
$\mathrm{Ru_2}(DMBA)_4(\mathrm{C_2Fc})_2{}^{20}$	2.4386(9)	1.979[9]	2.042[7]	1.195[11]	169.2[3]

$^a\mathrm{X} = \mathrm{Cl}$; $^b\mathrm{X} = \mathrm{F\text{-}BF_3^-}$; $^c\mathrm{X} = \mathrm{O\text{-}NO_2^-}$.

similar to that of $\mathrm{Ru_2}(hpp)_4\mathrm{Cl_2}$(2.321 Å).[41] The Ru-X distances are relatively long in all cases, indicating a weak Ru-X interaction. Both the short Ru-Ru bond and elongated Ru-X bonds are consistent with the retention of Ru-Ru σ-bonding, and a possible ground state configuration of $\sigma^2\pi^4\delta^2\pi^{*2}$.[25]

All *bis*-alkynyl adducts of the $\mathrm{Ru_2}(DMBA)_4$ core are diamagnetic molecules and exhibit well resolved [1]H and [13]C NMR spectra.[39] Most of the *bis*-adducts can be readily crystallized and characterized with single crystal diffraction study, and the structure of $\mathrm{Ru_2}(DMBA)_4(\mathrm{C_2SiMe_3})_2$ is shown in Figure 10. Structural study reveals a narrow range of Ru-Ru bond lengths (2.439–2.456 Å), which is similar to that of *ap*-based *bis*-adducts, but significantly shorter than that of *D*Ar*F*-based compounds. Structural distortion observed for other *bis*-adducts is also present in the *DMBA*-based species but to a lesser degree, as reflected by the smaller deviation from linearity in Ru-Ru-C$_\alpha$ angles.

Compounds containing the $\mathrm{Ru_2}(DMBA)_4$ core all exhibit at least three one-electron couples, which can be assigned according to Eq.(3). As shown by the representative CVs in Figure 11, $\mathrm{Ru_2}(DMBA)_4\mathrm{Cl_2}$ has the most positive couples, while the alkynyl adducts show dramatic cathodic shifts in the corresponding couples. Close examination of Figure 11 also revealed that the potentials of $\mathrm{Ru_2}(DMBA)_4(\mathrm{C_4SiMe_3})_2$ are slightly more positive than that of $\mathrm{Ru_2}(DMBA)_4(\mathrm{C_2SiMe_3})_2$, which is attributed to the more electron deficient nature of butadiynyl ligand compared to the ethynyl ligand.[39] It was also noted that the alkynyl-adducts of the $\mathrm{Ru_2}(DMBA)_4$ core are less stable toward redox processes in comparison with those of the $\mathrm{Ru_2}(D\mathrm{Ar}F)_4$ and $\mathrm{Ru_2}(ap)_4$ cores.[39] The E_g of *bis*-alkynyl adducts ranges between 1.6–1.7 V, while the E_op derived from the NIR absorption spectra ranges between 1.39–1.45 eV.

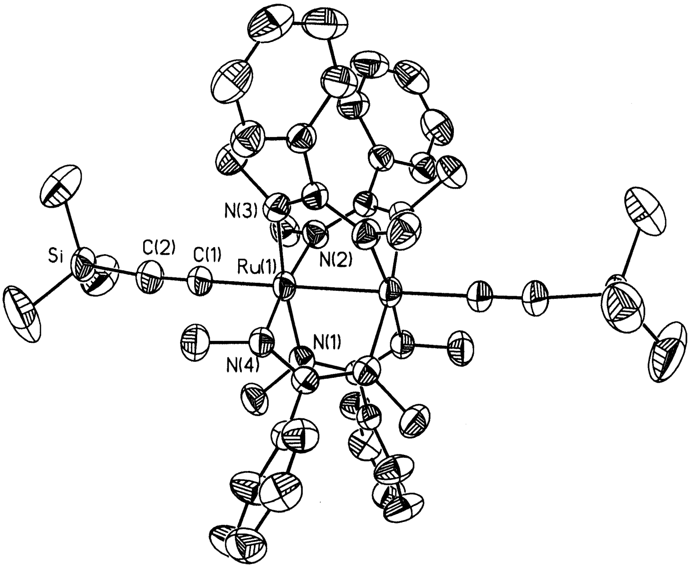

FIGURE 10 ORTEP plot of Ru_2(*DMBA*)$_4$(C_2SiMe_3)$_2$ at 30% probability level.

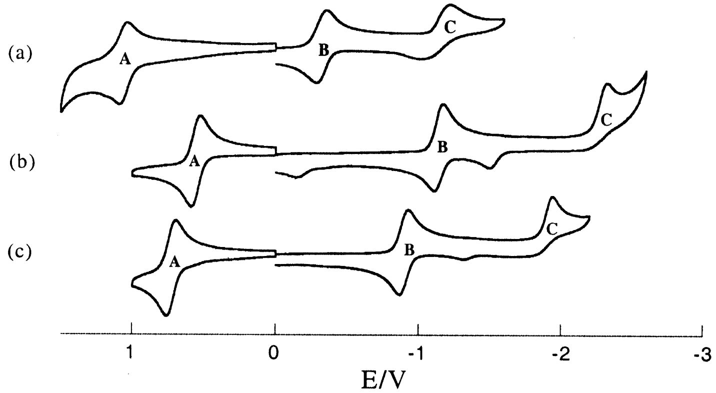

FIGURE 11 CVs of Ru_2(*DMBA*)$_4$$Y_2$, Y = Cl (a), C_2SiMe_3 (b) and C_4SiMe_3 (c).

5. DIMERIZED AND FC-CAPPED RU$_2$-METALLAYNES AND ELECTRONIC DELOCALIZATION THEREIN

A key prerequisite for conjugated oligomers to function as molecular wires is high electron mobility along the backbone. In oligo(Ru_2-metallayne), **II**,

TABLE 4 Oxidation/Reduction Potentials and Solution Electrochemical and Optical HOMO-LUMO Gaps for $\mathrm{Ru_2}$-metallaynes[a]

	$E_{1/2}(\mathbf{A})$/V	$E_{1/2}(\boldsymbol{B})$/V	$E_{1/2}(\boldsymbol{C})$/V	E_g/V[d]	E_op/eV[e]
$D\mathrm{Ar}F$-based compounds					
$\mathrm{Ru_2}(D\mathrm{Ph}F)_4(\mathrm{C_2Ph})$[b15]	—	0.33	−0.89	1.22	1.08
$\mathrm{Ru_2}(Dm\mathrm{ClPh}F)_4(\mathrm{C_2Ph})$[c]	—	0.74	−0.48	1.22	1.10
$\mathrm{Ru_2}(D\mathrm{mAni}F)_4(\mathrm{C_4SiMe_3})$[19]	—	0.63	−0.63	1.26	1.08
$\mathrm{Ru_2}(D\mathrm{mAni}F)_4(\mathrm{C_6SiMe_3})$[20]	—	0.68	−0.55	1.23	1.05
$\mathrm{Ru_2}(D\mathrm{Ph}F)_4(\mathrm{C_2Ph})_2$[b15]	0.73	−0.61	−1.54	1.34	1.25
$\mathrm{Ru_2}(Dm\mathrm{ClPh}F)_4(\mathrm{C_2Ph_2})_2$[c]	1.21	−0.19	−1.23	1.40	1.28
$\mathrm{Ru_2}(D\mathrm{mAni}F)_4(\mathrm{C_4SiMe_3})_2$[19]	1.17	−0.32	−1.32	1.49	1.35
$\mathrm{Ru_2}(Dm\mathrm{ClPh}F)_4(\mathrm{C_4SiMe_3})_2$[20]	1.28	−0.07	−1.06	1.35	1.29
ap-Based compounds					
$\mathrm{Ru_2}(ap)_4(\mathrm{C_2Ph})$[12]	—	0.19	−1.04	1.23	1.69
$\mathrm{Ru_2}(ap)_4(\mathrm{C_2SiMe_3})$[29]	—	0.20	−1.02	1.22	1.66
$\mathrm{Ru_2}(ap)_4(\mathrm{C_2H})$[29]	—	0.20	−1.03	1.23	1.66
$\mathrm{Ru_2}(ap)_4(\mathrm{C_2CH_2OCH_3})$[29]	—	0.20	−1.05	1.25	1.66
$\mathrm{Ru_2}(ap)_4(\mathrm{C_2SiMe_3})$[c]	—	0.45	−0.86	1.31	1.66
$\mathrm{Ru_2}(ap)_4(\mathrm{C_4SiMe_3})$[32]	—	0.48	−0.74	1.22	1.63
$\mathrm{Ru_2}(ap)_4(\mathrm{C_6SiMe_3})$[20]	—	0.50	−0.63	1.13	1.62
$\mathrm{Ru_2}(ap)_4(\mathrm{C_8SiMe_3})$[20]	—	0.54	−0.55	1.09	1.61
$\mathrm{Ru_2}(ap)_4(\mathrm{C_2Si^{\mathit{i}}Pr_3})$	—	0.46	−0.88	1.34	1.66
$\mathrm{Ru_2}(ap)_4(\mathrm{C_2Si^{\mathit{i}}Pr_3})$[20]	—	0.49	−0.74	1.23	1.63
$\mathrm{Ru_2}(ap)_4(\mathrm{C_6Si^{\mathit{i}}Pr_3})$[20]	—	0.52	−0.63	1.15	1.62
$\mathrm{Ru_2}(ap)_4(\mathrm{C_8Si^{\mathit{i}}Pr_3})$[20]	—	0.53	−0.56	1.09	1.61
$\mathrm{Ru_2}(ap)_4(\mathrm{C_2Ph})$[c]	—	0.44	−0.88	1.32	1.66
$\mathrm{Ru_2}(ap)_4(\mathrm{C_4Ph})$[20]	—	0.48	−0.74	1.22	1.64
$\mathrm{Ru_2}(ap)_4(\mathrm{C_6Ph})$[20]	—	0.50	−0.65	1.14	1.61
$\mathrm{Ru_2}(ap)_4(\mathrm{C_8Ph})$[20]	—	0.53	−0.55	1.08	1.61
$\mathrm{Ru_2}(ap)_4(\mathrm{C_{10}Ph})$[20]	—	0.54	−0.50	1.03	1.60
$\mathrm{Ru_2}(\mathrm{F_5}ap)_4(\mathrm{C_2Ph})$[b16]	—	0.80	−0.53	1.33	—
$\mathrm{Ru_2}(ap)_4(\mathrm{C_2Ph})_2$[31]	0.72	−0.42	−1.58	1.14	1.20
$\mathrm{Ru_2}(ap)_4(\mathrm{C_2SiMe_3})_2$[32]	0.90	−0.29	−1.38	1.19	1.19
trans-$(\mathrm{Me_3SiC_4})$-$[\mathrm{Ru_2}(ap)_4](\mathrm{C_2Si^{\mathit{i}}Pr_3})$[30]	0.84	−0.37	−1.49	1.21	1.19
trans-$(\mathrm{Me_3SiC_4})$-$[\mathrm{Ru_2}(ap)_4](\mathrm{C_2SiMe_3})$[30]	0.83	−0.36	−1.48	1.19	1.19
trans-$(\mathrm{HC_4})$-$[\mathrm{Ru_2}(ap)_4](\mathrm{C_2Si^{\mathit{i}}Pr_3})$[30]	0.84	−0.38	−1.54	1.22	1.20
trans-$(\mathrm{HC_4})$-$[\mathrm{Ru_2}(ap)_4](\mathrm{C_2SiMe_3})$[30]	0.83	−0.38	−1.51	1.21	1.20
trans-$(\mathrm{HC_4})[\mathrm{Ru_2}(ap)_4](\mathrm{C_2H})$[30]	0.83	−0.39	−1.53	1.22	1.21

(*Continued*)

TABLE 4 (*Continued*)

	$E_{1/}$(**A**)/V	$E_{1/2}$(***B***)/V	$E_{1/2}$(***C***)/V	E_g/V^d	E_{op}/eV^e
trans-(PhC_2)-$[Ru_2(ap)_4](C_2SiMe_3)^{31}$	0.75	−0.43	−1.62	1.18	1.20
trans-(PhC_2)-$[Ru_2(ap)_4](C_2SiMe_3)^{31}$	0.80	−0.35	−1.49	1.15	1.20
$Ru_2(F_5ap)_4(C_2Ph_2)_2{}^{b16}$	0.90	−0.05	−1.18	0.95	1.47
DMBA-based compounds					
$Ru_2(DMBA)_4Cl_2{}^{39}$	1.06	−0.32	−1.12	1.38	1.68
$Ru_2(DMBA)_4(C_2SiMe_3)_2{}^{39}$	0.56	−1.14	−2.32	1.70	1.42
$Ru_2(DMBA)_4(C_2H)_2{}^{39}$	0.57	−1.20	—	1.77	1.45
$Ru_2(DMBA)_4(C_2Ph)_2{}^{39}$	0.52	−1.10	—	1.62	1.39
$Ru_2(DMBA)_4(C_4SiMe_3)_2{}^{39}$	0.73	−0.90	−1.94	1.63	1.40
$Ru_2(DMBA)_4(C_4H)_2{}^{39}$	0.73	−0.92	−1.95	1.65	1.42
$Ru_2(DMBA)_4(C_2Fc)_2{}^{20}$	0.35	−1.16	—	1.51	1.39
$Ru_2(DMBA)_4(C_6Ph)_2{}^{20}$	0.80	−0.76	−1.69	1.56	1.42

[a] Unless specified, all CV data were recorded in 0.20 M THF solution of Bu_4NPF_6 *vs*. Ag/AgCl.

[b] Recorded in CH_2Cl_2 *versus* SCE, see the original references.

[c] Data reported in the original study were measured in CH_2Cl_2. Data reported here were re-measured in THF for the comparison purpose.

[d] $E_g = E_{1/2}(1+/0) - E_{1/2}(0/1-) = E_{1/2}(\mathbf{A}) - E_{1/2}(\mathbf{B})$ for the *bis*-adduct, and $E_{1/2}(\mathbf{B}) - E_{1/2}(\mathbf{C})$ for the *mono*-adduct.

[e] $E_{op}/eV = 10^7/(8066\lambda_{max}))$.

the backbone consists of alternating Ru_2 and polyyne-diyl units, and facile electron transfer across both components is essential for achieving high overall mobility. To probe the electron transfer efficiency along the polyyne-diyl chain, we have synthesized a series of $[Ru_2(ap)_4]_2(\mu\text{-}C_{2m})$ type compounds by either treating $Ru_2(ap)_4Cl$ with 0.5 equivalent of $LiC_{2m}Li$ ($m = 1$ and 2)[42] or *homo*-coupling of $Ru_2(ap)_4(C_mH)$ ($m = 4$ and 6) under *Hay/Eglington* conditions (Scheme 6).[20] Crystal structures of both $[Ru_2(ap)_4]_2(\mu\text{-}C_4)$[42] and $[Ru_2(ap)_4]_2(\mu\text{-}C_8)$[36] have been determined and the structural plots are shown in Figure 12.

The degree of electronic delocalization in these bridged molecules can be easily assessed by comparing the CV of $[Ru_2(ap)_4]_2(\mu\text{-}C_{2m})$ with that of its "half" molecule $Ru_2(ap)_4(C_mY)$ (m = even). One such comparison can be made based on Figure 13, where the CVs of $[Ru_2(ap)_4]_2(\mu\text{-}C_4)$ and $Ru_2(ap)_4(C_2SiMe_3)$ are shown. Between −1.5 and +1.3 V, the "half" molecule $Ru_2(ap)_4(C_2SiMe_3)$ undergoes two reversible one electron processes: an oxidation (**B**) and a reduction (**C**) in addition to an irreversible oxidation

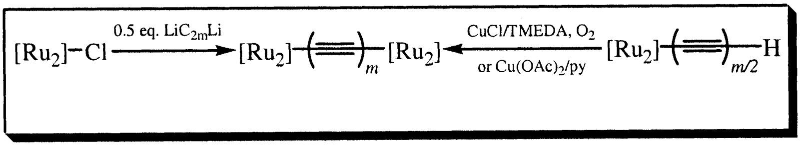

SCHEME 6 Synthesis of $[Ru_2(ap)_4]_2(\mu\text{-}C_{2m})$.

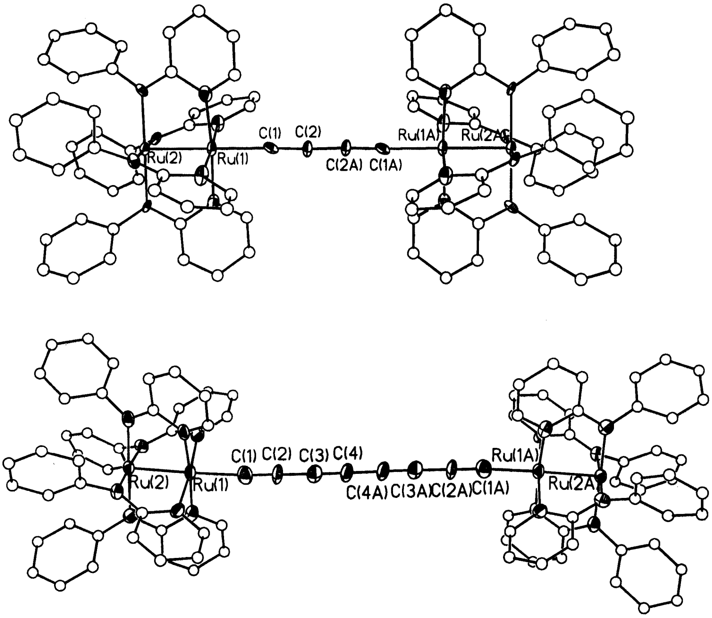

FIGURE 12 ORTEP plots of $[Ru_2(ap)_4]_2(\mu\text{-}C_4)$ (top) and $[Ru_2(ap)_4]_2(\mu\text{-}C_8)$ at 30% probability levels.

(**A**, not shown). The dimer, $[Ru_2(ap)_4]_2(\mu\text{-}C_4)$, displays four reversible one-electron couples: two oxidations (**B1** and **B2**, see Scheme 7 for the assignment) of potentials close to that of **B**, and two reductions (**C1** and **C2**) of potentials close to that of **C**. The pair-wise appearance of one-electron couples in the dimer clearly indicates that the strong electronic coupling between two $Ru_2(ap)_4$ cores enable a *collective* redox response. Furthermore, the potential splitting between **C1** and **C2** is quite large (0.389 V), which corresponds to a formal comproportionation constant for the monoanion $\{[Ru_2]_2\}^{1-}$ (K_{com}) of 3.8×10^6,[42] indicating that the monoanion *may* belong to the class III mixed valence compounds.[43] Interestingly, the splitting between **B1** and **B2** (0.157 V) is significantly smaller, and corresponds to a

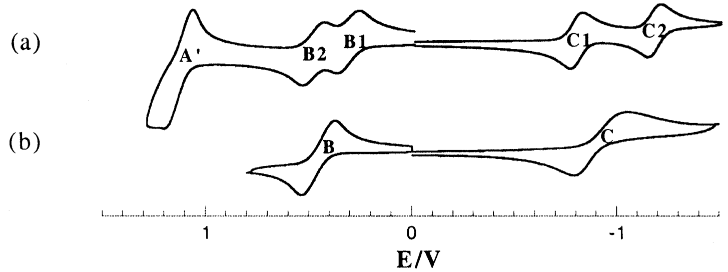

FIGURE 13 CVs of (a) $[Ru_2(ap)_4]_2(\mu\text{-}C_4)$ and (b) $Ru_2(ap)_4(C_2SiMe_3)$.

$$\{[Ru_2]_2\}^{4+} \overset{\mathbf{A'}}{\underset{+2e^-}{\overset{-2e^-}{\rightleftharpoons}}} \{[Ru_2]_2\}^{2+} \overset{\mathbf{B2}}{\underset{-e^-}{\overset{+e^-}{\rightleftharpoons}}} \{[Ru_2]_2\}^{1+} \overset{\mathbf{B1}}{\underset{-e^-}{\overset{+e^-}{\rightleftharpoons}}} [Ru_2]_2 \overset{\mathbf{C1}}{\underset{-e^-}{\overset{+e^-}{\rightleftharpoons}}}$$

$$\{[Ru_2]_2\}^{1-} \overset{\mathbf{C2}}{\underset{-e^-}{\overset{+e^-}{\rightleftharpoons}}} \{[Ru_2]_2\}^{2-} \overset{\mathbf{D1}}{\underset{-e^-}{\overset{+e^-}{\rightleftharpoons}}} \{[Ru_2]_2\}^{3-} \overset{\mathbf{D2}}{\underset{-e^-}{\overset{+e^-}{\rightleftharpoons}}} \{[Ru_2]_2\}^{4-}$$

SCHEME 7 Assignment of redox couples in $[Ru_2(ap)_4]_2(\mu\text{-}C_{2m})$.

$K_{com}(\{[Ru_2]_2\}^{1+})$ of 506. The contrast between two K_{com}s clearly indicates that the Ru_2-polyynyl system is a much better electron carrier than a hole carrier, and this behavior can be attributed to the electron-deficient nature of both the Ru_2 core and butadiynyl bridge.

Availability of $[Ru_2(ap)_4]_2(\mu\text{-}C_{2m})$ with $m = 1$, 2, 4, and 6 facilitates the study of the dependence of electron delocalization on the length of the polyynediyl bridge. CV's of these compounds recorded between -3.0 and $+1.5$ V are shown in Figure 14, where several trends are apparent. First, the oxidation couples **B1** and **B2** that are clearly resolved with the C_2 and C_4 bridges merge into a pseudo two-electron wave with the C_8 bridge, and become a standard two-electron wave with the C_{12} bridge. A similar trend holds for the pair of **C1** and **C2** couples, where the splitting gradually reduces as the chain elongates, but the two couples remained resolved up to C_{12} bridge. These trends are consistent with the general consensus that the degree of electron coupling decays exponentially as the distance increases.[43] A quasi-reversible two-electron wave (**A′**) was detected at very positive potential with C_2 and C_4 bridges, but not with longer bridges, where the increasing electron

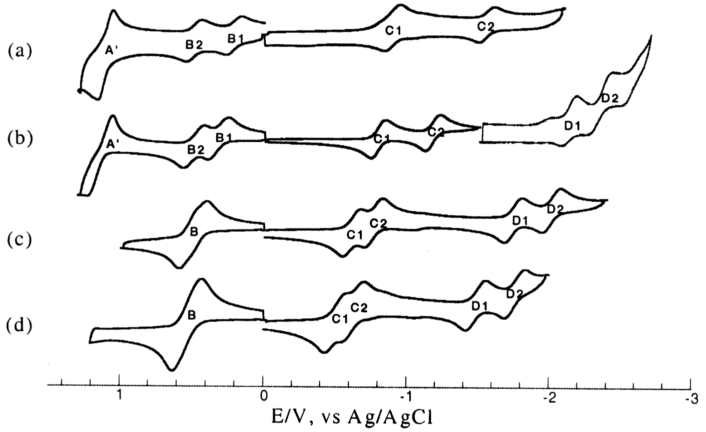

FIGURE 14 CVs of (b) $[Ru_2(ap)_4]_2(\mu\text{-}C_2)$, (b) $[Ru_2(ap)_4]_2(\mu\text{-}C_4)$, and (c) $[Ru_2(ap)_4]_2$-$(\mu\text{-}C_8)$, and (d) $[Ru_2(ap)_4]_2(\mu\text{-}C_{12})$.

deficiency has shifted the couple out of the potential window accessible in THF ($\leq +1.5$ V). Also of interest is the emergence of a second pair of one-electron reductions at more negative potentials, marked as **D1** and **D2**. These appear at very negative potentials (< -2 V) with the C_4 bridge, and shift anodically as the chain lengthens. Intriguingly, the potential splitting between **D1** and **D2** remains almost a constant as the chain length varies, contradicting the trends observed for the **B** and **C** pairs. Finally, the C_4-bridged compound exhibits six one-electron couples and one two-electron couple, which is extremely unusual for a single molecule.

To explore the ability of the Ru_2 core to facilitate electron transfer, $Ru_2(DMBA)_4(C_2Fc)_2$, shown in Figure 15, was synthesized and structurally characterized. Its CV is shown in Figure 16, where four one electron couples are apparent between -1.5 and $+1.5$ V. Tentative assignment of the observed couples are two Ru_2-based, **B** and **C**, and two ferrocenyl-based, **Fc1** and **Fc1**, which implies a potential splitting of *ca.* 300 mV between the latter pair. This large splitting reflects the strong electronic coupling between two Fc units mediated by the $Ru_2(DMBA)_4$ core, and its magnitude, comparable to that observed for 1,1′-biferrocene,[44] is remarkable considering the edge-edge distance between two ferrocenyls is about 11.2 Å in $Ru_2(DMBA)_4(C_2Fc)_2$.

6. CONCLUSIONS AND OUTLOOK

We have demonstrated that diruthenium-polyynyl complexes can be synthesized and they generally exhibit remarkable stability towards air, heat and moisture. These compounds undergo multiple one electron redox

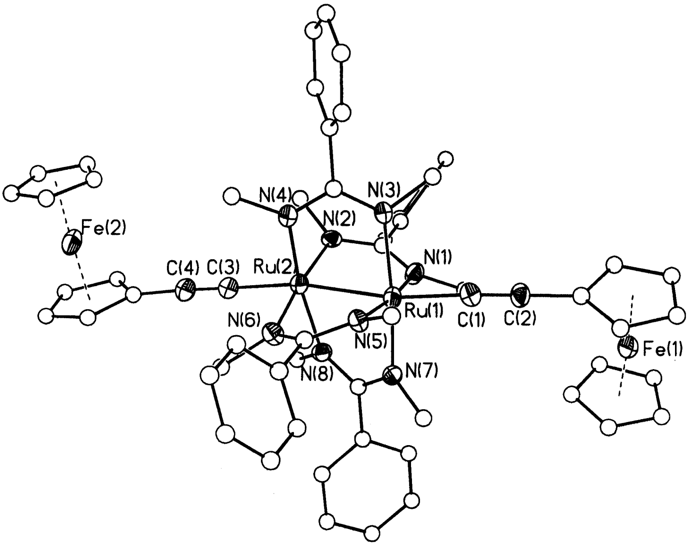

FIGURE 15 ORTEP plot of $Ru_2(DMBA)_4(C_2Fc)_2$ at 30% probability level.

processes and thus qualify themselves as electron reservoirs. Furthermore, electrochemical and spectroscopic data reveal the presence of both small HOMO-LUMO gaps and high electron affinity for the *bis*-alkynyl species, two requisites that are critical for the building blocks of *molecular wires*. The three types of *N,N′*-bidentate supporting ligands employed differentiate in the electron-richness of the resultant Ru_2-metallaynes in the following order: *DMBA* > *ap* > *D*ArF. Phenyl-substituted derivatives of *DMBA* and *D*Ar*F* ligands can be readily synthesized and hence facilitate both the electronic and solubility tunings of Ru_2-metallaynes. Preliminary studies indicate that

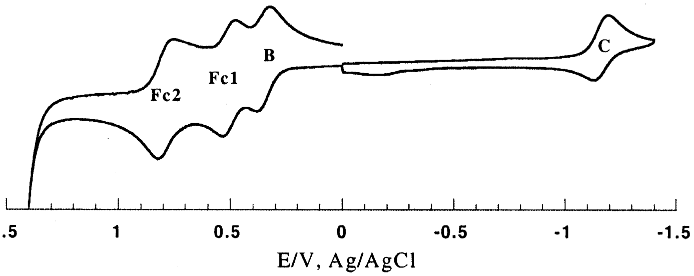

FIGURE 16. CV of $Ru_2(DMBA)_4(C_2Fc)_2$.

Ru_2-metallynes with ≡C-H terminus can be either *homo*-coupled, or *cross*-coupled with HC≡CY under either *Hay* or *Eglington* conditions. Our current efforts are directed towards in-depth understanding of the mechanism and controlled oligomerization of Ru_2-metallaynes.

While Ru_2-metallynes described here are designed for the construction of linear oligomer **II**, the same synthetic strategy can also be applied to generate branched oligomers. Based on the success in synthesizing dendrimer of mononuclear Ru-complexes,[45] one may visualize the branched analogs of $Ru_2(ap)_4(C_2Ph)$, where the phenylacetylide ligand is replaced with either 1,3-diethynylbenzene or 1,3,5-triethynylbenzene ligand. Recent work of Kuhn *et al*. demonstrated the feasibility of obtaining linear heterometallic assembly with suitable linear ditopic ligands.[22] Considering the propensity of linear ditopic ligands, more related work should emerge in near future. Assembling supramolecules based on M-M bonded dimetallic units with linkers other than polyyne-diyls has been a fast expanding area, where successfully incorporated dimetallic units include Mo_2, W_2, Rh_2, and Re_2.[46,47] Both Rh_2 and Re_2 systems are known to exhibit high affinity towards axial ligands and it would be interesting to see whether polyynyl ligands can be exploited in these systems.

ACKNOWLEDGMENTS

We thank both the University of Miami and the Petroleum Research Fund/ACS (36595-AC3) for their support, and Professor John Fackler, Jr. for encouragement and patience. The authors also benefit greatly from stimulating discussions with Professors Al Cotton and Angel Kaifer.

REFERENCES

1. Low, P. J. and M. I. Bruce. 2001. *Adv. Organomet. Chem.* 48, 71.
2. Manna, J., K. D. John and M. D. Hopkins. 1995. *Adv. Organomet. Chem.* 38, 79.
3. (a) Whittall, I. R., A. M. McDonagh, M. G. Humphrey and M. Samoc. 1998. *Adv. Organomet. Chem.* 42, 291; (b) ibid, 1999. 43, 349.
4. Yam, V. W.-W. 2001. *Chem. Comm.* 789.
5. For highlights and reviews on organometallic molecular wires, see (a) Paul, F. and C. Lapinte. 1998. *Coord. Chem. Rev.* 178–180, 431; (b) Chisholm, M. H. 1991. *Angew. Chem., Int. Ed. Engl.* 30, 673; (c) Lang, H. 1994. *Angew. Chem. Int. Ed. Engl.* 33, 547; (d) Bunz, U. H. F. 1996. *Angew. Chem. Int. Ed. Engl.* 35, 969; (e) Halpern, J. 2001. *Pure Appl. Chem.* 73, 209.
6. Bruce, M. I., P. J. Low, K. Costuas, J.-F. Halet, S. P. Best and G. A. Heath. 2000. *J. Am. Chem. Soc.* 122, 1949.
7. Dembinski, R., T. Bartik, B. Bartik, M. Jaeger and J. A. Gladysz. 2000. *J. Am. Chem. Soc.* 122, 810.
8. Kheradmandan, S., K. Heinze, H. W. Schmalle and H. Berke. 1999. *Angew. Chem. Int. Ed. Engl.* 38, 2270.

9. Le Narvor, N., L. Toupet and C. Lapinte. 1995. *J. Am. Chem. Soc.* 117, 7129.
10. Schwab, P. F. H., M. D. Levin and J. Michl. 1999. *Chem. Rev.* 99, 1863.
11. (a) Roncali, J. 1997. *Chem. Rev.* 97, 173; (b) Wada, Y., M. Tsukada, M. Fujihira, K. Matsushige, T. Ogawa, M. Haga and S. Tanaka. 2000. *Jpn. J. Appl. Phys. Part 1* 39, 3835.
12. Chakravarty, A. R. and F. A. Cotton. 1986. *Inorg. Chim. Acta* 113, 19.
13. Yao, C. L., K. H. Park, A. R. Khokhar, M. J. Jun and J. L. Bear. 1990. *Inorg. Chem.* 29, 4033.
14. (a) Stoner, T. C., R. F. Dallinger and M. D. Hopkins. 1990. *J. Am. Chem. Soc.* 112, 5651; (b) Stoner, T. C., S. J. Geib and M. D. Hopkins. 1992. *J. Am. Chem. Soc.* 114, 4201; (c) Stoner, T. C., S. J. Geib and M. D. Hopkins. 1993. *Angew. Chem. Int. Ed. Engl.* 32, 409; (d) Stoner, T. C., W. P. Schaefer, R. E. Marsh and M. D. Hopkins. 1994. *J. Cluster Sci.* 5, 107; (e) John, K. D., T. C. Stoner and M. D. Hopkins. 1997. *Organometallics* 15, 4948; (f) John, K. D., V. M. Miskowski, M. A. Vance, R. F. Dallinger, L. C. Wang, S. J. Geib and M. D. Hopkins. 1998. *Inorg. Chem.* 37, 6858.
15. (a) Bear, J. L., B. Han and S. Huang. 1993. *J. Am. Chem. Soc.* 115, 1175; (b) Bear, J. L., B. Han, S. Huang and K. M. Kadish. 1996. *Inorg. Chem.* 35, 3012.
16. Bear, J. L., Y. Li, B. Han, E. V. Caemelbecke and K. M. Kadish. 1997. *Inorg. Chem.* 36, 5449.
17. (a) Lin, C., T. Ren, E. J. Valente and J. D. Zubkowski. 1999. *J. Organomet. Chem.* 579, 114; (b) Lin, C., T. Ren, E. J. Valente and J. D. Zubkowski. 1998. *J. Chem. Soc., Dalton Trans.* 571.
18. Cotton, F. A. and R. A. Walton. 1993. *Multiple Bonds between Metal Atoms*. Oxford: Oxford University Press.
19. Xu, G. and T. Ren. 2001. *Inorg. Chem.* 40, 2925.
20. Ren, T. and G. Xu. unpublished results.
21. Wong, K.-T., J.-M. Lehn, S.-M. Peng and G.-H. Lee. 2000. *Chem. Commun.* 2259.
22. Zuo, J.-L., E. Herdtweck and F. E. Kühn. 2002. *J. Chem. Soc., Dalton Trans.* 1244.
23. Cotton, F. A. and T. Ren. 1995. *Inorg. Chem.* 34, 3190.
24. Lin, C. 1997. Ph.D. Dissertation Thesis, Florida Institute of Technology.
25. Cotton, F. A. and A. Yokochi. 1997. *Inorg. Chem.* 36, 567.
26. Carey, F. A. and R. J. Sundberg. 1990. *Advanced Organic Chemistry*. New York: Plenum.
27. Ren, T. 1998. *Coord. Chem. Rev.* 175, 43.
28. Loutfy, R. O. and R. O. Loutfy. 1976. *Can. J. Chem.* 54, 1454.
29. Zou, G., J. C. Alvarez and T. Ren. 2000. *J. Organomet. Chem.* 596, 152.
30. Ren, T. 2002. *Organometallics* 21, 732.
31. Xu, G. and T. Ren. 2002. *J. Organomet. Chem.* 655, 239.
32. Xu, G. and T. Ren. 2001. *Organometallics* 20, 2400.
33. Cotton, F. A., S. E. Stiriba and A. Yokochi. 2000. *J. Organomet. Chem.* 595, 300.
34. Siemsen, P., R. C. Livingston and F. Diederich. 2000. *Angew. Chem. Int. Ed. Engl.* 39, 2632.
35. Bartik, B., R. Dembinski, T. Bartik, A. M. Arif and J. A. Gladysz. 1997. *New J. Chem.* 21, 739.
36. Ni, Y. 2001. MS. Thesis, University of Miami.
37. Chakravarty, A. R., F. A. Cotton and D. A. Tocher. 1985. *Inorg. Chem.* 24, 172.
38. Launay, J.-P. 2001. *Chem. Soc. Rev.* 30, 386.
39. Xu, G., C. Campana and T. Ren. 2002. *Inorg. Chem.* 41, 3521.
40. (a) Touchard, D. and P. H. Dixneuf. 1998. *Coord. Chem. Rev.* 178–180, 409; (b) Puerta, M. C. and P. Valerga. 1999. *Coord. Chem. Rev.* 193–195, 977.

41. Bear, J. L., Y. Li, B. Han and K. M. Kadish. 1996. *Inorg. Chem*. 35, 1395.
42. Ren, T., G. Zou and J. C. Alvarez. 2000. *Chem. Comm*. 1197.
43. (a) Brunschwig, B. S., C. Creutz and N. Sutin. 2002. *Chem. Soc. Rev*. 31, 168; (b) Crutchley, R. J. 1994. *Adv. Inorg. Chem*. 41, 273.
44. Levanda, C., K. Bechgaard and D. O. Cowan. 1976. *J. Org. Chem*. 41, 2700.
45. (a) Hurst, S. K., M. P. Cifuentes and M. G. Humphrey. 2002. *Organometallics* 21, 2353; (b) Whittall, I. R., M. G. Humphrey, S. Houbrechts, J. Maes, A. Persoons, S. Schmid and D. C. R. Hockless. 1997. *J. Organomet. Chem*. 544, 277; (c) Long, N. J., A. J. Martin, F. F. d. Biani and P. Zanello. 1998. *J. Chem. Soc., Dalton Trans*. 2017.
46. For recent reviews see: (a) Cotton, F. A., C. Lin and C. A. Murillo. 2001. *Acc. Chem. Res*. 34, 759; (b) Cotton, F. A., C. Lin and C. A. Murillo. 2002. *Proc. Nat. Acad. Sci., USA* 99, 4810; (c) Eglin, J. L. 2002. *Comments Inorg. Chem*. 23, 23.
47. For recent research articles see: (a) Kuang, S. M., P. E. Fanwick and R. A. Walton. 2002. *Inorg. Chem*. 41, 147; (b) Kuang, S. M., P. E. Fanwick and R. A. Walton. 2002. *Inorg. Chem*. 41, 405; (c) Bera, J. K., R. Clerac, P. E. Fanwick and R. A. Walton. 2002. *J. Chem. Soc., Dalton Trans*. 2168; (d) Xue, W. M. and F. E. Kuhn. 2001. *Eur. J. Inorg. Chem*. 2041.